Int. J. Heat Mass Transfer. Vol. 25, No. 10, pp. 1559–1568, 1982
Printed in Great Britain

0017-9310/82/101559-10 $03.00/0
Pergamon Press Ltd.

NATURAL CONVECTION BETWEEN HORIZONTAL CONCENTRIC CYLINDERS WITH DENSITY INVERSION OF WATER FOR LOW RAYLEIGH NUMBERS

T. HUNG NGUYEN, P. VASSEUR and L. ROBILLARD
Department of Civil Engineering, Ecole Polytechnique, Université de Montréal, Montréal, H3C 3A7, Canada

(*Received* 6 *July* 1981 *and in final form* 11 *February* 1982)

Abstract—A study is made of the natural convection of cold water between two horizontal concentric cylinders with constant surface temperatures. The governing equations are solved by the perturbation method and the solutions are expressed as power series of the nonlinear Rayleigh number. The flow patterns and heat transfer rates are presented in terms of the radius ratio R, the nonlinear Rayleigh number Ra, and the inversion parameter γ which essentially determines the size and effects of the additional convection cells that arise from the inversion of density of water at 4°C within the cavity. Good agreement is obtained with the existing numerical and experimental results.

NOMENCLATURE

$\mathbf{e}_r$, $\mathbf{e}_\phi$, unit vectors in the cylindrical coordinate system;
g', gravitational acceleration;
Nu, Nusselt number, $-\ln R\left(r\dfrac{\partial T}{\partial r}\right)$;
$\overline{Nu}$, average Nusselt number, $\dfrac{1}{\pi}\displaystyle\int_0^\pi Nu\,\mathrm{d}\phi$;
p, pressure;
Pr, Prandtl number;
r, ϕ, radial and angular cylindrical coordinates;
R, radius ratio, r'_o/r'_i;
Ra, Rayleigh number, $g'\beta'_2 r'^3_i(T'_i - T'_o)^2/\nu'\alpha'$;
Ra_G, Rayleigh number based on the gap width, $g'\beta'_2(r'_o - r'_i)^3\,(T'_i - T'_o)^2/\nu'\alpha'$;
Ra_n, nth Rayleigh number;
T, temperature;
U, V, velocity components in the r and ϕ directions, respectively;
$\mathbf{V}$, total velocity.

Greek symbols

α', thermal diffusivity;
β'_n, volumetric coefficient of expansion, equation (1);
γ, inversion factor, $\beta'_1/\beta'_2\,(T'_i - T'_o)$;
ε, coefficient in the expansion of the average Nusselt number, $(\overline{Nu} - 1)/Ra_G^2$;
ν', kinematic viscosity;
ρ, density;
Ψ, stream function.

Subscripts

i, inner cylinder;
o, outer cylinder;
r, reference state.

Superscript

denotes dimensional variables.

INTRODUCTION

BUOYANCY induced flows of cold water are a very common occurrence in nature and technology. The mechanism of such flows is considerably complicated by the fact that the density of water reaches a maximum value at about 4°C. Since the pioneering works of Ede [1] and Merk [2], the problem of natural convection of cold water has received increasing interest not only because of the fundamental importance of the density inversion phenomenon, but also because of its various practical applications. For instance, Desai and Forbes [3], Watson [4], and Robillard and Vasseur [5] have investigated numerically the problem of a rectangular cavity with isothermal vertical walls and insulated horizontal ones, and found that the resulting flow as well as the heat transfer can significantly differ from that of a common fluid with a linear density–temperature relationship. For example, instead of the familiar unicellular pattern, the flow in cold water can become bicellular, and the average Nusselt number goes through a minimum value when the two convective cells are of approximately the same size. These results have been confirmed in the experiments of Seki *et al.* [6]. Also, the transient behaviour of a mass of water cooled down under various thermal boundary conditions through the point of maximum density has been investigated numerically by Forbes and Cooper [7], Vasseur and Robillard [8], and Robillard and Vasseur [9] for the case of a rectangular cavity, and by Cheng *et al.* [10, 11], and Gilpin [12] for a horizontal circular pipe. All these studies have shown that the flow can be greatly influenced by the presence of a maximum density which will eventually reverse the initial circulation inside the cavity, and considerably reduces

the heat transfer compared with the case of a common fluid.

In this paper, an analytical study is made of the convection of cold water contained between two horizontal concentric cylinders with constant surface temperatures. The purpose of this study is twofold. The first is to obtain an analytical solution using the regular perturbation method. This solution, within its range of validity, has the advantage of providing an exhaustive view of the inversion phenomenon, and of predicting the trend of its evolution as the various parameters of the problem change. Although a numerical approach might be more practical, a systematic analysis of this problem would, however, require a considerable investment in cost and time due to the fact that, as will be discussed later, at least one additional parameter is involved in the description of a fluid characterized by a nonlinear equation of state. The second purpose of this study is to present an analytical solution which can readily be used as a basis for future numerical studies of flow regimes lying beyond the range of validity of this theory. Also, it should be noted that our interest in this problem has stemmed from the experimental work of Seki *et al.* [13] who investigated the flow patterns and heat transfer of cold water between two cylinders with a radius ratio varying from 1.18 to 6.39, and a temperature of the outer cylinder varying from 1 to 15°C, the inner cylinder being kept at 0°C. To our knowledge, no analytical study has been made of this problem although the convection of an ordinary fluid in a horizontal cylindrical annulus has been extensively investigated by many authors [14–20]; a comprehensive bibliography can be found in the paper by Kuehn and Goldstein [21].

BASIC EQUATIONS

The problem under consideration is that of 2-dim. steady laminar convection in a cylindrical annulus.

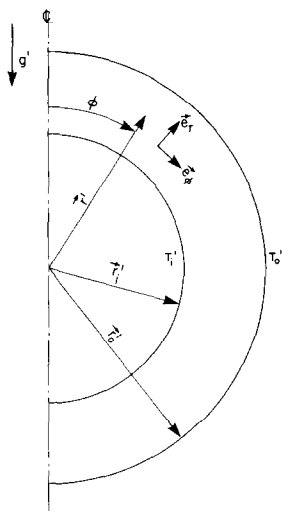

FIG. 1. Flow geometry and coordinate system.

The geometry of the problem is shown in Fig. 1. The gap between the cylinders is filled with a viscous fluid which is set in motion by the temperature difference across the annulus. The inner and outer cylinders, of radii r_i' and r_o', are maintained at temperatures T_i' and T_o', respectively. All fluid properties, except the specific weight, are taken to be constant and are evaluated at the mean temperature $\bar{T}' = (T_i' + T_o')/2$. A discussion on this approximation can be found in the paper by Mack and Bishop [18]. To determine the buoyancy force, the following equation of state will be used:

$$\rho' = \rho_r' \left[1 - \sum_{n=1}^{N} \beta_n' (T' - T_r')^n \right] \quad (1)$$

where ρ' and T' are the density and temperature of the fluid, β_n's are the expansion coefficients, and the subscript r designates a reference state.

It should be noted that the above equation of state is quite general and can be applied, in principle, to a large variety of fluids by appropriately choosing the values of n, the degree of the polynomial, and β_n', the corresponding expansion coefficients. For example, in the case of an ordinary fluid with a linear density–temperature relationship, $n = 1$ and the value of β_1' is a characteristic constant of the fluid under consideration. On the other hand, water at low temperature is characterized not only by the fact that the relationship between its density and temperature is nonlinear, but essentially because it presents a maximum density at 3.98°C. A few other fluids, like bismuth, antimony and gallium are also affected by a similar anomaly. The solutions developed in the present study can be applied to these fluids provided that their corresponding expansion coefficients are used. For the case of water at low temperature it should also be mentioned that various approximations of the equation of state have been proposed in the past. For example, when considering the temperature range 0–20°C, third and fourth degree polynomials have been used by Vanier and Tien [24], and Fujii [25], respectively. In this study, a second degree polynomial will be used, such that

$$\rho' = \rho_r' [1 - \beta_1' (T' - T_r') - \beta_2' (T' - T_r')^2] \quad (2)$$

with $\beta_1' = 2(T_r' - T_m')\,\beta_2'$, $\beta_2' = 8 \times 10^{-6} °C^{-2}$ and $T_m' = 3.98°C$. The density given by this equation agrees with the experimental value to 1 part per million (p.p.m.) in the temperature range 2–6°C, and to 5 p.p.m. in the range 0–2°C and 6–8°C. The buoyancy force is thus determined with an accuracy better than 4% over the range 0–8°C [22, 23].

Although the use of the above equation of state has the disadvantage of limiting its validity to the range of approximately 0–8°C, this is largely compensated by the fact that one can predict all the essential features associated with an inversion of density by introducing just one more parameter as compared with a classical situation of an ordinary fluid without inversion of density. In fact, for the general case of a fluid with a

nonlinear equation of state, the present problem is governed by four independent parameters, namely r'_i, r'_o, T'_i and T'_o (besides the Prandtl number which will be considered as a characteristic constant of the fluid). However, by choosing a second degree equation of state, as given by equation (2), it is found that the number of governing parameters is reduced to three, namely, R, $Ra_1 = g'\beta'_1 r'^3_i (T'_i - T'_o)/\alpha'\nu'$ and $Ra_2 = g'\beta'_2 r'^3_i (T'_i - T'_o)^2/\alpha'\nu'$ while a fluid characterized by a linear equation of state is governed by only two well-known parameters R and Ra_1. Since in equation (2) β'_i is a function of T'_o while β'_2 is a characteristic constant of the fluid, it follows that Ra_1 depends on both T'_i and T'_o while Ra_2 depends only on the temperature difference $(T'_i - T'_o)$ as in the case of the Rayleigh number for an ordinary fluid. This suggests that one should choose Ra_2 as the appropriate Rayleigh number, and define a nonlinear Rayleigh number

$$Ra \equiv Ra_2 \tag{3}$$

together with a second parameter

$$\gamma = \frac{Ra_1}{Ra_2} = \frac{-2(T'_m - T'_o)}{T'_i - T'_o}. \tag{4}$$

This parameter γ, hereafter called the inversion parameter, relates the temperature for maximum density T'_m to the wall temperatures. (A similar parameter has been used by Carey *et al.* [26] to study the effects of inversion on the boundary layer of cold pure and saline water at a vertical isothermal surface.) When $-2 < \gamma < 0$, T'_m lies in the range of the fluid temperature and there exists an inversion of density within the confined fluid. The special value $\gamma = -1$ corresponds to the case where T'_m is in the middle of the range of the fluid temperature, and the fluid density on the inner cylinder is the same as that on the outer one. This particular case will be referred in the present study as the case of 'complete inversion'. When $\gamma \leqslant -2$ or $\gamma \geqslant 0$, no inversion will be observed and the flow approaches that of a common fluid when $|\gamma| \gg 1$.

By using the above equation of state to determine the buoyancy force in the spirit of the Boussinesq approximation, the set of the continuity, momentum and energy equations can be transformed to the following coupled system for the dimensionless stream function and temperature:

$$\frac{\partial}{\partial t}\nabla^2\Psi = Pr\nabla^4\Psi - \frac{1}{r}\left(\frac{\partial\Psi}{\partial\phi}\frac{\partial\nabla^2\Psi}{\partial r} - \frac{\partial\Psi}{\partial r}\frac{\partial\nabla^2\Psi}{\partial\phi}\right) + Pr\left(\frac{\cos\phi}{r}\frac{\partial}{\partial\phi} + \sin\phi\frac{\partial}{\partial r}\right)\sum_{n=1}^{N} Ra_n T^n, \tag{5}$$

$$\frac{\partial T}{\partial t} + \frac{1}{r}\left(\frac{\partial\Psi}{\partial\phi}\frac{\partial T}{\partial r} - \frac{\partial\Psi}{\partial r}\frac{\partial T}{\partial\phi}\right) = \nabla^2 T. \tag{6}$$

For the case of isothermal rigid boundaries, and due to the symmetry of the flows with respect to the vertical plane passing through the axis of the cylinders, the above system of equations must satisfy the following conditions:

$$\Psi = \frac{\partial\Psi}{\partial r} = 0 \quad \text{at } r = 1, R, \tag{7a}$$

$$\Psi = \frac{\partial^2\Psi}{\partial\phi^2} = 0 \quad \text{at } \phi = 0, \pi, \tag{7b}$$

$$T = 1 \quad \text{at } r = 1, \tag{8a}$$

$$T = 0 \quad \text{at } r = R, \tag{8b}$$

$$\frac{\partial T}{\partial\phi} = 0 \quad \text{at } \phi = 0, \pi. \tag{8c}$$

In the following section, the nonlinear system (5)–(6) will be solved for small values of the Rayleigh number using the perturbation method.

PERTURBATION SOLUTIONS

The series solutions

For small values of the Rayleigh number Ra, one can express the solutions of the system of equations (5) and (6) in the form of power series of Ra, such that

$$T = \sum_{m=1}^{\infty} Ra^{m-1} T_m, \tag{9}$$

$$\Psi = \sum_{m=1}^{\infty} Ra^m T_m. \tag{10}$$

By substituting equations (9) and (10) into equations (5) and (6) and equating terms of the same order in Ra, one readily obtains the following hierarchy of linear inhomogeneous equations:

$$\nabla^2 T_1 = 0, \tag{11a}$$

$$\nabla^4\Psi_1 = \left(-\cos\phi\frac{\partial}{r\partial\phi} - \sin\phi\frac{\partial}{\partial r}\right)(\gamma T_1 + T_1^2), \tag{11b}$$

$$\nabla^2 T_2 = \frac{1}{r}\left(\frac{\partial T_1}{\partial r}\frac{\partial\Psi_1}{\partial\phi} - \frac{\partial T_1}{\partial\phi}\frac{\partial\Psi_1}{\partial r}\right), \tag{12a}$$

$$\nabla^4\Psi_2 = \left(-\cos\phi\frac{\partial}{r\partial\phi} - \sin\phi\frac{\partial}{\partial r}\right)(\gamma T_2 + 2T_1 T_2) + \frac{1}{rPr}\left(\frac{\partial\nabla^2\Psi_1}{\partial r}\frac{\partial\Psi_1}{\partial\phi} - \frac{\partial\nabla^2\Psi_1}{\partial\phi}\frac{\partial\Psi_1}{\partial r} - \frac{\partial\nabla^2\Psi_1}{\partial\Phi}\frac{\partial\Psi_1}{\partial r}\right), \tag{12b}$$

$$\nabla^2 T_3 = \frac{1}{r}\left(\frac{\partial T_1}{\partial r}\frac{\partial\Psi_2}{\partial\phi} - \frac{\partial T_1}{\partial\phi}\frac{\partial\Psi_2}{\partial r} + \frac{\partial T_2}{\partial r}\frac{\partial\Psi_1}{\partial\phi} - \frac{\partial T_2}{\partial\phi}\frac{\partial\Psi_1}{\partial r}\right), \tag{13a}$$

$$\nabla^4\Psi_3 = \left(-\cos\phi\frac{\partial}{r\partial\phi} - \sin\phi\frac{\partial}{\partial r}\right) \times (\gamma T_3 + T_2^2 + 2T_1 T_3) + \frac{1}{rPr}$$

$$\times\left(\frac{\partial\nabla^2\Psi_1}{\partial r}\frac{\partial\Psi_2}{\partial\phi}-\frac{\partial\nabla^2\Psi_1}{\partial\phi}\frac{\partial\Psi_2}{\partial r}\right.$$

$$\left.+\frac{\partial\nabla^2\Psi_1}{\partial r}\frac{\partial\Psi_1}{\partial\phi}-\frac{\partial\nabla^2\Psi_2}{\partial\phi}\frac{\partial\Psi_1}{\partial r}\right). \quad (13b)$$

The corresponding boundary conditions are

$$\Psi_m=\frac{\partial\Psi_m}{\partial r}=0 \quad \text{at } r=1, R, \quad (14a)$$

$$\Psi_m=\frac{\partial^2\Psi_m}{\partial\phi^2}=0 \quad \text{at } \phi=0, \pi, \quad (14b)$$

$$T_1=1 \quad \text{at } r=1, \quad (15a)$$

$$T_1=0 \quad \text{at } r=R, \quad (15b)$$

$$T_m=0 \quad \text{at } r=1, R, \quad (15c)$$

$$\frac{\partial T_m}{\partial\phi}=0 \quad \text{at } \phi=0, \pi. \quad (15d)$$

For practical purposes, the series (9) and (10) will be approximated by the first three terms such that

$$T=T_1+Ra\,T_2+Ra^2\,T_3, \quad (16)$$

$$\Psi=Ra\Psi_1+Ra^2\Psi_2+Ra^3\Psi_3. \quad (17)$$

Using the method of separation of variables, one can solve successively the hierarchy of equations (11)–(13) and obtain solutions of the form

$$T_m=\sum_{i,j,k}A_m(i,j,k)r^{i-m}\ln r^{j-1}\cos(k-1)\phi, \quad (18)$$

$$\Psi_m=\sum_{i,j,k}B_m(i,j,k)r^{i-m-1}\ln r^{j-1}\sin k\phi \quad (19)$$

where the summations are over indices i, j and k, and the coefficients $A_m(i,j,k)$ and $B_m(i,j,k)$ are, in general, functions of the parameters Pr, R and γ. In particular, the first coefficients $A_1(i,j,k)$, $A_2(i,j,k)$, $A_3(i,j,1)$ and $B_1(i,j,k)$ are functions of R and γ only, i.e. to the lowest order in the Rayleigh number, the flow patterns and isotherms are independent of the Prandtl number. For reference purposes, these coefficients are given in the Appendix. Readers interested in other coefficients, which have been stored in a computer memory to save space, are invited to write to the authors.

Validity of the series expansions

Before discussing the results obtained from the above solutions, it should be noted that these expansions in power series of Ra *do not* converge uniformly. In fact, when $R\to\infty$, they will diverge no matter how small the Rayleigh number may be. For finite values of the radius ratio R, one can expect, but not prove, that the series will converge in a certain range of the Rayleigh number. The reliability of the truncated series then depends on how fast they will converge. Physically speaking, as these series represent a perturbation of a pure conduction state, they must be close to the true solution when the heat transfer by convection is "small" compared to that due to conduction: This condition can be expressed in term of the average Nusselt number as

$$\overline{Nu}<1.25 \quad (20)$$

which implies that the second term in the expression of the average Nusselt number (due to convection) must be at least four times smaller than the first one (due to conduction).

In term of the Rayleigh number, condition (20) can be expressed, by virtue of equation (24), as

$$Ra_G<\frac{1}{2\varepsilon^{1/2}} \quad (21)$$

where ε is a function of R and γ as determined from the second order temperature T_2 [see equation (25) below].

When condition (20) or (21) is satisfied, one can reasonably expect that the truncated series (16) and (17) will represent the true solution to within several percent.

The family of curves in Fig. 2 shows the limiting value of Ra_G below which the series solutions are reliable. It should be noted that all these curves correspond to a same Nusselt number $\overline{Nu}=1.25$, and therefore indicate the required Rayleigh number to achieve a same degree of convection for various values of R and γ.

RESULTS AND DISCUSSION

The series expansions (16) and (17) have been evaluated numerically for various combinations of the dimensionless parameters, R, Ra and γ. It was found necessary to perform the numerical calculations with double precision as has been pointed out by Mack and Bishop [18]. To expedite plotting of the results, an auxiliary computer program was used to locate points lying on specified isotherms and streamlines. Due to the symmetry of the geometry of this problem, it was found convenient to represent the computer results on a single graph with the flow pattern on the right half of the cavity and the isotherms on the left half. Note that in all these graphs, the increments between adjacent isotherms and streamlines are respectively $\Delta T=(T_i-T_o)/5=0.2$ and $\Delta\Psi=(|\Psi_{max}|+|\Psi_{min}|)/5$, Ψ_{max} and Ψ_{min} being the values of the stream functions at the centers of the clockwise and counterclockwise vortices, respectively.

Effects of inversion

For fixed values of R and Ra, the inversion phenomenon is governed by the parameter γ which relates the position of the maximum of density to the walls of the cavity. The value of γ can be varied by changing both T'_o and T'_i such that $T'_i-T'_o$ remains constant. As mentioned earlier, the particular value $\gamma=-1$ corresponds to the case of complete inversion with a zero density difference between the two cylinders, and a mean temperature $(T'_i+T'_o)/2$ equal to the temperature at maximum density. Typical results for various

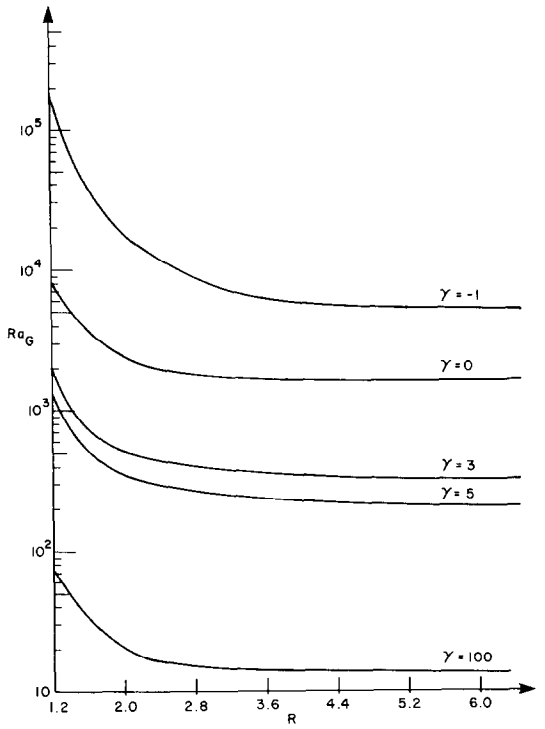

FIG. 2. Maximum Rayleigh number for the validity of the truncated series solutions.

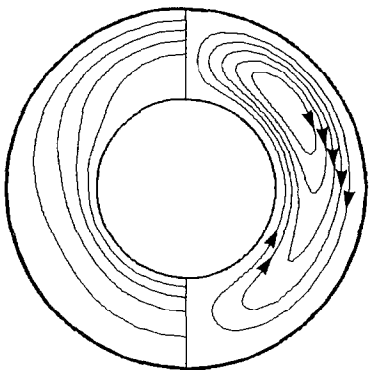

FIG. 3(a). Streamlines and isothermals for $Ra = 2000, R = 2$ and $\gamma = 0$ and $\Psi_{max} = 4.6$.

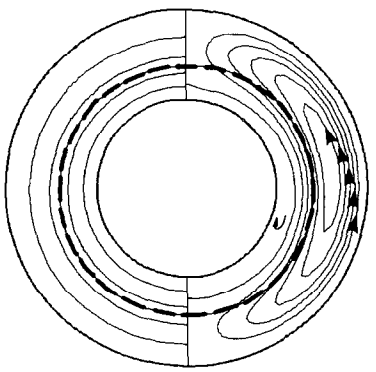

FIG. 3(b). Streamlines and isothermals for $Ra = 2000, R = 2$ and $\gamma = -1$, $\Psi_{max} = -0.045$ and $\Psi_{min} = -0.71$.

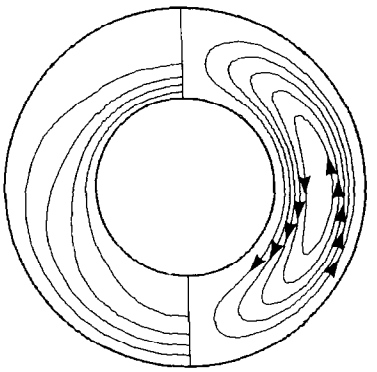

FIG. 3(c). Streamlines and isothermals for $Ra = 2000, R = 2$ and $\gamma = -2$ and $\Psi_{min} = -4.8$.

values of γ, with $R = 2$ and $Ra = 2000$, are presented in Figs. 3(a)–(c) and 4(a) and (b). Figure 3(a) shows the flow and isotherm patterns when the maximum of density is situated at the outer cylinder, corresponding to $\gamma = 0$. The flow then consists of two symmetrical (with respect to the vertical axis) counterrotating vortices with a downward motion near the outer cylinder. One notes that the flow pattern is of a tadpole shape lying in the upper part of the annulus where the fluid motion is the strongest. The maximum heat transfer, occurs, however, both at the top of the outer cylinder and at the bottom of the inner one. Since there is no density inversion in this case, the flow is similar to that observed in an ordinary fluid [14–21].

The case of complete inversion, with $\gamma = -1$, is shown in Fig. 3(b) where the heavy dashed line represents the 4°C isotherm corresponding to the region of maximum density. In the neighborhood of this region, the fluid moves downward while near both the inner and outer cylinders, its upward motion results in the appearance of two counterrotating vortices in each half of the cavity. This effect of inversion is responsible for the sharp cut of the heat transfer rate as indicated by the almost concentric isotherms (Fig. 3b) in comparison with the rather distorted pattern of the previous case (Fig. 3a). As far as the heat transfer mechanism is concerned, the complete inversion case is thus characterized by a pseudo-conduction regime as defined by Grigull and Hauf [27].

Figure 3(c) shows the flow and isotherm patterns when the maximum density is situated at the inner cylinder, corresponding to $\gamma = -2$. In this case, the fluid motion as well as the isotherm patterns are opposite to that observed in Fig. 3(a). Here, it is interesting to remark that although the convection is still weak, one can already see the development of two thermal boundary layers at the inner and outer cylinders, respectively. To illustrate the effects of inversion on the relative intensity and direction of the convective motion, the angular velocity is represented in Fig. 4(a) for the three typical values of γ considered above while more detailed flow field in the case of

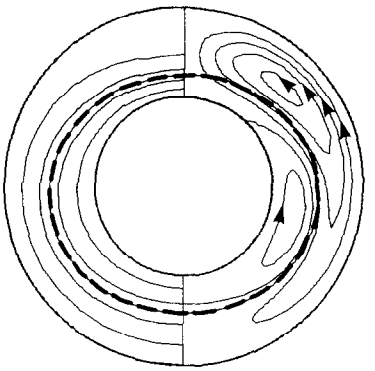

FIG. 3(d). Streamlines and isothermals for $Ra = 8000$, $R = 2$ and $\gamma = -1$, $\Psi_{max} = 1.1$ and $\Psi_{min} = -2.7$.

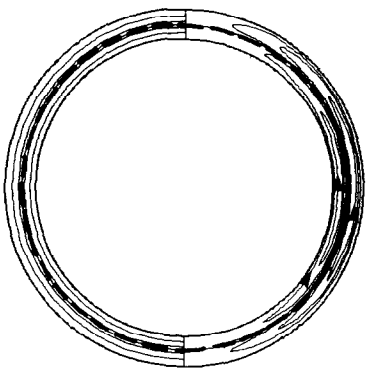

FIG. 3(f). Streamlines and isothermals for $Ra = 8000$, $R = 1.2$ and $\gamma = -1$, $\Psi_{max} = 0.0087$ and $\Psi_{min} = -0.013$.

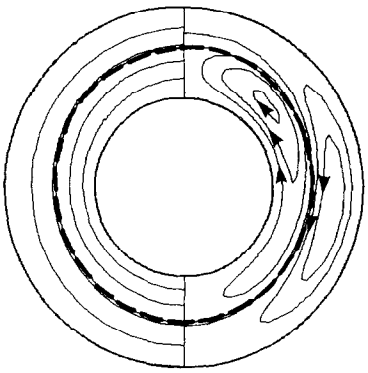

FIG. 3(e). Streamlines and isothermals for $Ra = 8000$, $R = 2$ and $\gamma = -0.857$, $\Psi_{max} = 1.5$ and $\Psi_{min} = -1.4$.

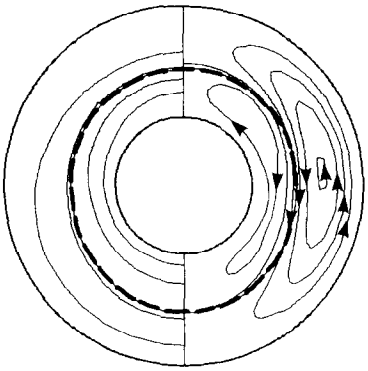

FIG. 3(g). Streamlines and isothermals for $Ra = 8000$, $R = 2.6$ and $\gamma = 0.857$, $\Psi_{max} = 3.2$ and $\Psi_{min} = -6.7$.

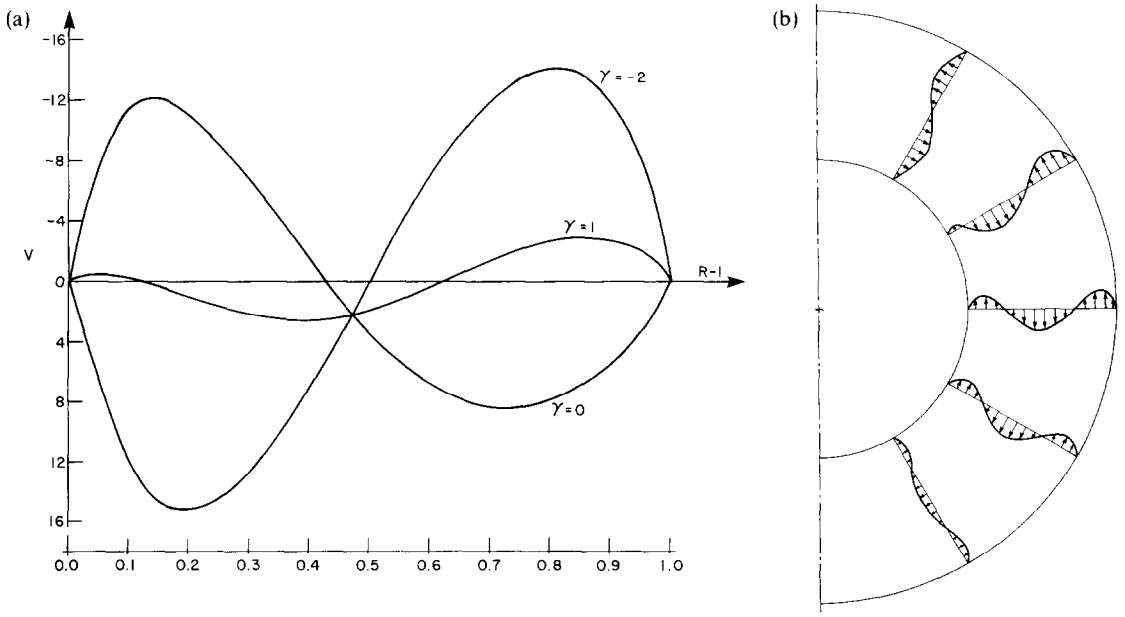

FIG. 4(a). Angular velocity profiles at $\phi = 90°$ for $Ra = 8000$, $R = 2$ with γ as a parameter.
FIG. 4(b). Angular velocity profiles for $Ra = 8000$, $R = 2$ and $\gamma = -1$ at various angular positions.

complete inversion is illustrated in Fig. 4(b) by the angular velocity at various positions within the annulus.

Effects of the Rayleigh number and the radius ratio

Effects of the Rayleigh number on the inversion phenomenon are shown in Figs. 3(b) and 3(d), corresponding respectively to $Ra = 2000$ and 8000. From these figures one can see that by increasing the Rayleigh number, the inner cell is pushed down while the outer one moves up and gradually changes from the well-known kidney shape to that of a tadpole. Also, the convection is enhanced in such a way that the isotherms are squeezed to the top of the inner cylinder, and to the bottom of the outer one.

Effects of the radius ratio on the inversion phenomenon can be seen from Figs. 3(d) and (f) or Figs. 3(e) and (g) which show that for small values of R (i.e. $R - 1 \leqslant 1$) the two counterrotating cells (in the case of complete inversion) are approximately of the same size and of the classical crescent eddy type. As R is increased, the flow and isotherm patterns change qualitatively in a same way as with an increasing Rayleigh number. When no inversion of density is present in the cavity, it is found that for $\gamma \geqslant 0$ the unicellular flow, corresponding to the inner cell in the previous case, moves up as R (or Ra) is increased while the isotherms get closer to each other at the top of the outer cylinder and at the bottom of the inner one. A completely reverse situation is observed when $\gamma \leqslant -2$. These observations are in agreement with past literature on the convection of ordinary fluids [21].

Heat transfer rates

The local heat transfer rates at the inner and outer cylinders can be expressed in terms of the corresponding local Nusselt numbers Nu_i and Nu_o defined by

$$Nu_{i,o} = -\ln R \left[r \frac{\partial T}{\partial r} \right]_{r=1,R} \tag{22}$$

with $T = T_1 + RaT_2 + Ra^2 T_3$ as calculated in the previous section.

A study of the local Nusselt numbers readily shows that the maximum (as well as the minimum) heat transfer rates are localized around the vertical axis of the annulus (i.e. at $\phi = 0$ and π) as previously observed from the isotherm patterns.

While the local Nusselt numbers indicate the distribution of the heat flow across a given surface, the total heat flow across that surface is given by the overall (or average) Nusselt number as defined by

$$\overline{Nu} = \frac{1}{\pi} \int_0^{\pi} Nu_{i,o} \, d\phi \tag{23}$$

(where, by virtue of the balance of energy, the integration over the inner and outer surfaces must be the same).

Expressions for $\overline{Nu}$ can be shown to have the form

$$\overline{Nu} = 1 + \varepsilon Ra_G^2 \tag{24}$$

where Ra_G is the Rayleigh number based on the gap width, and

$$\varepsilon = -(R-1)^{-6} \ln R \sum_i A_3 \, (i, 2, 1). \tag{25}$$

Here, it should be noted that ε is a function of R and γ only, and therefore, to the lowest order in the Rayleigh number, the overall heat transfer rate is independent of the Prandtl number.

Within its range of validity, equation (24) explicitly shows that the overall Nusselt number is made up of two terms, the first of which represents the heat transfer due to pure conduction while the second one arises from the heat transfer by convection. The family of curves in Fig. 5 describes the effects of density inversion, for various values of R, on the overall convective heat transfer coefficient $\varepsilon = (\overline{Nu} - 1)/Ra_G^2$. All these curves present a very sharp minimum in the neighborhood of the value $\gamma = -1$, thereby indicating a sharp cut of the heat transfer rate due to the complete inversion of the fluid density. For example, the minimum value of ε at $\gamma \simeq -1$ is about 10^3 times smaller than its value at $\gamma = -2$ (i.e. in the absence of inversion). This implies that for a given difference of temperature $\Delta T' = T_i' - T_o'$ across the annulus, the heat transfer due to convection can be reduced by a factor of 10^3 by changing the temperature of the inner cylinder from, say, $T_i' = T_m'$ to $T_i' \simeq T_m' + \frac{1}{2}\Delta T'$. This sharp cut is essentially due to the presence of two counterrotating vortices that arise from the inversion of the fluid density, and is one of its most significant effects on the mechanism of heat transfer by convection within an enclosure. Finally, it should be noted that the family of curves in Fig. 5 is universal, and can be used to determine the overall heat transfer rate of any fluid as specified by a set of parameters R, γ and Ra.

Comparison with existing results

Although no analytical study has been made of the present problem, many results have been published for the case of ordinary fluids with a linear equation of state. For instance, Mack and Bishop [18], on the basis of the perturbation method, have studied the case of ordinary gases ($Pr = 0.7$) as well as that of liquid metals ($Pr = 0.02$). All their results can be reproduced from the present solutions by letting $|\gamma| \to \infty$, and keeping γRa fixed. Also, Custer and Shaughnessy [19] have studied the convection of liquid metals by using double regular expansions in powers of the Rayleigh and Prandtl numbers. Both constant temperatures and constant heat flux were imposed on the boundaries. Again, their results for the case of constant wall temperatures can be readily obtained from the present solutions by letting $Pr \to 0$, $|\gamma| \to \infty$, and keeping γRa fixed. Finally, we have reproduced the results for some of the cases studied by Crawford and Lemlich [14] ($R = 8$, $Ra_1 = 9$, $Pr = 0.714$), Powe *et al.* [15] ($R = 1.57$, $Ra_1 = 13\,348$, $Pr = 0.7$ and $R = 1.2$; $Ra_1 = 345\,920$, $Pr = 0.7$) and Kuehn and Goldstein [21] ($R = 1.2$, $Ra_1 = 10^4$, $Pr = 0.7$; $R = 2.6$, $Ra_1 = 1000$, $Pr = 0.7$).

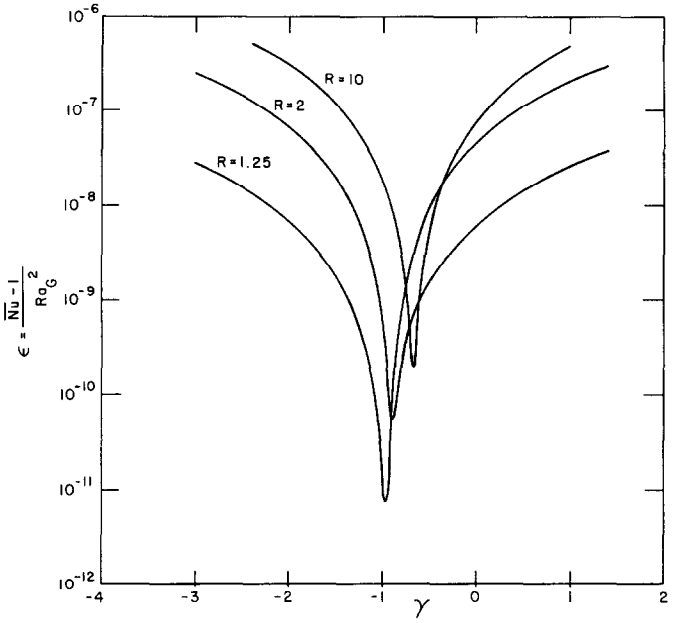

FIG. 5. Coefficient of convective heat transfer, $\varepsilon = (\overline{Nu} - 1)/Ra_G^2$ as a function of γ and R.

The current analysis predicted essentially identical results for the isotherms, flow patterns and, to within a few percent, the average Nusselt number.

In the case of a fluid with inversion of density, numerical and experimental studies of the present problem have been obtained by Seki *et al.* [13, 28], and by Vasseur *et al.* [29]. While the numerical solutions in the latter study agree satisfactorily with ours, the results published by Seki *et al.* [13, 28] correspond to Rayleigh numbers lying generally beyond the range of validity of the present theory and cannot be compared directly with our results. However, it is more significant to note that the essential features associated with the inversion phenomenon as described in the previous section are consistent with the experimental observations, and, therefore, can be used to predict the trend of the flow patterns and heat transfer for convective regimes lying beyond the range of validity of this theory.

CONCLUSIONS

The solution to the problem of natural convection of cold water contained in a horizontal annulus has been obtained by the regular perturbation method. The density–temperature curve of water around 4°C has been approximated by a parabola to describe the phenomenon of density inversion. The problem then was shown to depend on three dimensionless parameters R, Ra and γ, representing the radius ratio, the nonlinear Rayleigh number, and the inversion parameter, respectively. An analysis of the flow patterns and heat transfer rates showed that:

(1) For $|\gamma| \gg 1$ the present problem tends to that of an ordinary fluid with a linear equation of state, and all the well-known results can be obtained from the present solutions by taking the limit $|\gamma| \to \infty$ and keeping γ Ra fixed and equal to the classical linear Rayleigh number.

(2) For $-2 < \gamma < 0$, the maximum density temperature $T'_m = 4°C$ is situated between the cylinder temperatures and there exists an inversion of density within the confined fluid. In the limit case $\gamma = -2$ (i.e. $T'_i = 4°C$) a unicellular counterclockwise flow is present inside the cavity and the maximum heat transfer occurs at the top of the inner cylinder and at the bottom of the outer one. In the other limit case $\gamma = 0$ the situation is completely reversed. For $-2 < \gamma < 0$ the flow pattern consists of two counterrotating cells in each half of the annulus, the inner cell being always clockwise and the outer one always counterclockwise. For $-2 < \gamma < -1$ the dominant cell is the outer one and moves from the lower part of the annulus to the upper part as γ is increased. For $-1 < \gamma < 0$ the dominant cell is the inner one and its center also moves up as γ tends towards zero. The presence of two counterrotating cells inside the cavity is essentially due to the inversion of the fluid density which can effectively cut the heat transfer down to the level of almost pure conduction such that, as γ approaches -1 from either 0 or -2, the isotherms become more and more concentric circles. This was clearly shown by the presence of a very sharp minimum of the curve representing the overall Nusselt number in term of the inversion parameter.

(3) The effects of increasing the Rayleigh number and/or the radius ratio on the inversion phenomenon is twofold. First, the convection inside the cavity is enhanced with a flow pattern gradually changing from a crescent shape to that of a tadpole, by passing through the well-known kidney shape. Second, the

inner cell is pushed down while the outer one moves up, tending to separate the flow into two thermal boundary layers.

(4) Finally, a comparison with the existing numerical and experimental results shows that, within its range of validity, the present theory faithfully predicts the essential features associated with the inversion of density, and can serve as a basis for future studies of this phenomenon at higher Rayleigh numbers.

Acknowledgements—This work was supported by the National Research Council of Canada through grants NRC A-9201 and NRC A-4197. The authors gratefully thank Ecole Polytechnique for providing the necessary time on an IBM 360/70 computer.

REFERENCES

1. A. J. Ede, Heat transfer by natural convection in refrigerated liquid, *Proc. 8th Int. Congr. Refrigeration*, London, p. 260 (1951).
2. H. J. Merk, The influence of melting and anomalous expansion on the thermal convection in laminar boundary layers, *Appl. Sci. Res.* **4**, 435–452 (1954).
3. V. S. Desai and R. E. Forbes, Free convection in water in the vicinity of maximum density, in *Environmental and Geophysical Heat Transfer*, pp. 41–47. ASME (1971).
4. A. Watson, The effect of the inversion temperature on the convection of water in an inclosed rectangular cavity, *Q. Jl Mech. Appl. Math.* **25**, 423–446 (1972).
5. L. Robillard and P. Vasseur, Effet du maximum de densité sur la convection libre de l'eau dans une cavité fermée *Can. J. Civil Engng* **6**, 481–493 (1979).
6. N. Seki, S. Fukusako and H. Inaba, Free conserved heat transfer with density inversion in a confined rectangular vessel, *Wärme-und Stoffübertragung* **11**, 145–156 (1978).
7. R. E. Forbes and J. W. Cooper, Natural convection in a horizontal layer of water cooled from above to near freezing, *Trans. Am. Soc. Mech. Engrs*, Series C, *J. Heat Transfer* **97**, 47–53 (1975).
8. P. Vasseur and L. Robillard, Transient natural convection heat transfer in a mass of water cooled through 4°C, *Int. J. Heat Mass Transfer* **23**, 1195–1205 (1980).
9. L. Robillard and P. Vasseur, Transient natural convection heat transfer of water with maximum density and supercooling, *Trans. Am. Soc. Mech. Engrs*, Series C, *J. Heat Transfer* **103**, 528–534 (1981). See also National Heat Transfer Conference, Orlando, Florida, ASME Paper No. 80-HT-74 (1980).
10. K. C. Cheng, M. Takeuchi and R. R. Gilpin, Transient natural convection in horizontal water pipe with maximum density effect and supercooling, *Num. Heat Transfer* **1**, 101–115 (1978).
11. K. C. Cheng and M. Takeuchi, Transient natural convection of water in a horizontal pipe with constant cooling rate through 4°C, *Trans. Am. Soc. Mech. Engrs*, Series C, *J. Heat Transfer* **98**, 581–587 (1976).
12. R. R. Gilpin, Cooling of a horizontal cylinder of water through its maximum density point at 4°C, *Int. J. Heat Mass Transfer* **18**, 1307–1315 (1975).
13. N. Seki, S. Fukusako and M. Nakaoka, Experimental study on natural convection heat transfer with density inversion of water between horizontal concentric cylinders, *Trans. Am. Soc. Mech. Engrs*, Series C, *J. Heat Transfer* **97**, 556–561 (1975).
14. L. Crawford and R. Lemlich, Natural convection in horizontal concentric cylindrical annuli, *IEC Fundamentals* **4**, 260–264 (1962).
15. R. E. Powe, C. T. Carley and S. L. Carruth, A numerical solution for natural convection in cylindrical annuli, *Trans. Am. Soc. Mech. Engrs*, Series C, *J. Heat Transfer* **93**, 210–220 (1971).
16. E. H. Bishop, C. T. Carley and R. E. Powe, Natural convection oscillatory flow in cylindrical annuli, *Int. J. Heat Mass Transfer* **11**, 1741–1752 (1968).
17. M. C. Charrier-Mojtabi, A. Mojtabi and J. P. Caltagirone, Numerical solution of a flow due to natural convection in horizontal cylindrical annulus, *Trans. Am. Soc. Mech. Engrs*, Series C, *J. Heat Transfer* **101**, 171–173 (1979).
18. L. R. Mack and E. H. Bishop, Natural convection between horizontal concentric cylinders for low Rayleigh numbers, *Q. Jl Mech. Appl. Math.* **2**, 223–241 (1968).
19. J. R. Custer and E. J. Shaughnessy, Thermoconvective motion of low Prandtl number fluids within a horizontal cylidnrical annulus, *Trans. Am. Soc. Mech. Engrs*, Series C, *J. Heat Transfer* **99**, 596–602 (1977).
20. J. Huetz and J. P. Petit, Natural and mixed convection in concentric annular spaces—experimental and theoretical results for liquid metals, *5th Int. Heat Transfer Conf.*, Tokyo, Vol. 3, pp. 169–172 (1974).
21. T. H. Kuehn and R. J. Goldstein, An experimental and theoretical study of natural convection in the annulus between horizontal cylinders, *J. Fluid Mech.* **74**, 695–719 (1976).
22. Landolt-Börnstein, *Zahlenwerte und Funktionem*, Vol. 2, pp. 36–37. Springer, Berlin (1971).
23. D. R. Moore and N. O. Weiss, Nonlinear penetrative convection, *J. Fluid Mech* **61**, 553–581 (1973).
24. C. R. Vanier and C. Tien, Effect of maximum density and melting on natural convection heat transfer from a vertical plate, *Chem. Engng Prog. Symp. Ser.* **82**, 240–254 (1968).
25. T. Fujii, Fundamentals of free convection heat transfer, *Prog. Heat Transfer Engng* **3**, 66–68 (1974).
26. V. P. Carey, B. Gebhart and J. C. Mollendorf, Buoyancy force reversals in vertical natural convection flows in cold water, *J. Fluid Mech.* **97**, 279–298 (1980).
27. U. Grigull and W. Hauf, Natural convection in horizontal cylindrical annuli, *3rd Int. Heat Transfer Conf.*, Chicago, pp. 182–195 (1966).
28. N. Seki, S. Fukusako and M. Nakaoka, An analysis of free convective heat transfer with density inversion of water between two horizontal concentric cylinders, *Trans. Am. Soc. Mech. Engrs*, Series C, *J. Heat Transfer* **98**, 670–672 (1976).
29. P. Vasseur, L. Robillard and B. Chandra Shekar, A numerical study on natural convection heat transfer with density inversion of water within a horizontal cylindrical annulus, *Nat. Heat Transfer Conf.*, Milwaukee, Wisconsin (1981).

APPENDIX

The coefficients $A_1(i,j,k)$, $A_2(i,j,k)$ and $B_1(i,j,k)$ appearing in equations (18) and (19) are functions of the radius ratio R and the inversion parameter γ as given in the following expressions (only non-zero coefficients will be written):

$$A_1(1,1,1) = a_1, \quad A_1(1,2,1) = a_2,$$
$$A_2(1,1,2) = a_3, \quad A_2(3,1,2) = a_4,$$
$$A_2(5,1,2) = a_5, \quad A_2(1,2,2) = a_6,$$
$$A_2(3,2,2) = a_7, \quad A_2(5,2,2) = a_8,$$
$$A_2(3,3,2) = a_9, \quad A_2(5,3,2) = a_{10},$$
$$B_1(1,1,1) = b_1, \quad B_1(3,1,1) = b_2,$$
$$B_1(5,1,1) = b_3, \quad B_1(3,2,1) = b_4,$$
$$B_1(5,2,1) = b_5, \quad B_1(5,3,1) = b_6,$$

where

$$b_6 = -\frac{\ln^{-2} R}{16},$$

$$b_5 = -\frac{\ln^{-1} R}{16}(2 - \ln^{-1} R + \gamma) + \frac{3\ln^{-2} R}{32},$$

$$b_4 = \left[\frac{1 - R^2 + 2R^2 \ln R}{(1 - R^2)^2} + \frac{(-1 + R^2 + 2R^2 \ln R)}{(1 + 2R^2 - 3R^4)}\right]^{-1} \times \left[\frac{(-1 + R^2 - 2R^4 \ln R)b_5 - (2R^4 \ln^2 R)b_6}{(1 - R^2)^2} + \frac{(1 + R^2 - 2R^4 - 6R^4 \ln R)b_5 - (4R^4 \ln R + 6R^4 \ln^2 R)b_6}{(1 + 2R^2 - 3R^4)}\right],$$

$$b_3 = -\tfrac{1}{2}(1 - R^2)^{-1}[(1 - R^2 + 2R^2 \ln R)b_4 + (1 - R^2 + 2R^4 \ln R)b_5 + (2R^4 \ln^2 R)b_6],$$

$$b_2 = -\tfrac{1}{2}(4b_3 + b_4 + b_5),$$

$$b_1 = -b_2 - b_3,$$

and

$$a_{10} = \frac{\ln^{-1} R}{8} b_6,$$

$$a_9 = \frac{\ln^{-1} R}{4} b_4,$$

$$a_8 = \frac{\ln^{-1} R}{8} b_5 - \frac{3\ln^{-1} R}{16} b_6,$$

$$a_7 = \frac{\ln^{-1} R}{2} b_2 - \frac{\ln^{-1} R}{4} b_4,$$

$$a_6 = -\frac{\ln^{-1} R}{2} b_1,$$

$$a_5 = \frac{\ln^{-1} R}{8} b_3 - \frac{3\ln^{-1} R}{32} b_5 + \frac{7\ln^{-1} R}{64} b_6,$$

$$a_4 = -(R^2 - 1)^{-1}[(R^4 - 1)a_5 + (a_6 + a_7 R^2 + a_8 R^4)\ln R + (a_9 R^2 + a_{10} R^4)\ln^2 R],$$

$$a_3 = -a_4 - a_5,$$

$$a_2 = -\ln^{-1} R,$$

$$a_1 = 1.$$

CONVECTION NATURELLE ENTRE DES CYLINDRES CONCENTRIQUES HORIZONTAUX AVEC INVERSION DE DENSITE DE L'EAU A DES FAIBLES NOMBRES DE RAYLEIGH

Résumé—On étudie la convection naturelle de l'eau froide entre deux cylindres horizontaux et concentriques avec des températures de surface constantes. Les équations de base sont résolues par la méthode de perturbation et les solutions sont exprimées en série puissance du nombre de Rayleigh non-linéaire. Les configurations de l'écoulement et les flux thermiques sont présentés en fonction du rapport des rayons R, du nombre de Rayleigh non-linéaire Ra, et le paramètre d'inversion γ qui déterminent essentiellement la taille et les effets des cellules de convection qui apparaissent dans la cavité à partir de l'inversion de densité de l'eau à 4°C. Un bon accord est obtenu avec les résultats numériques et expérimentaux existants.

FREIE KONVEKTION ZWISCHEN HORIZONTALEN KONZENTRISCHEN ZYLINDERN MIT DICHTE-INVERSION VON WASSER BEI KLEINEN RAYLEIGH-ZAHLEN

Zusammenfassung—Die freie Konvektion von kaltem Wasser zwischen zwei horizontalen konzentrischen Zylindern mit konstanter Oberflächentemperatur wird untersucht. Die wesentlichen Gleichungen werden mit Hilfe eines Störungsansatzes gelöst. Die Lösungen werden als Potenzreihe der nichtlinearen Rayleigh-Zahl ausgedrückt. Die Strömungsform und der Wärmeübergang werden durch das Radien-Verhältnis R und den Inversionsparameter γ dargestellt. Dieser bestimmt im wesentlichen Größe und Einfluß der zusätzlichen Konvektions-Zellen, die durch die Dichte-Inversion von Wasser bei 4°C in dem Hohlraum entstehen. Es zeigt sich eine gute Übereinstimmung mit bestehenden numerischen und experimentellen Ergebnissen.

ЕСТЕСТВЕННАЯ КОНВЕКЦИЯ МЕЖДУ ГОРИЗОНТАЛЬНЫМИ КОНЦЕНТРИЧЕСКИМИ ЦИЛИНДРАМИ С ИНВЕРСИЕЙ ПЛОТНОСТИ ВОДЫ ПРИ МАЛЫХ ЗНАЧЕНИЯХ ЧИСЛА РЕЛЕЯ

Аннотация—Проведено исследование естественной конвекции в слое холодной воды между двумя горизонтальными концентрическими цилиндрами, поверхность которых имеет постоянную температуру. Определяющие уравнения решаются методом возмущений, и решения выражаются в виде степенных рядов нелинейного числа Релея. Структура течения и интенсивность теплопереноса зависят от отношения радиусов R, нелинейного числа Релея Ra и параметра инверсии γ, который определяет размер и влияние дополнительных конвективных ячеек, возникающих из-за инверсии плотности воды при 4°C в зазоре между цилиндрами. Получено хорошее согласие с имеющимися численными и экспериментальными результатами.